Developmental Biology 405 (2015) 10–20

Contents lists available at ScienceDirect

Developmental Biology

journal homepage: www.elsevier.com/locate/developmentalbiology

Absence of catalytic domain in a putative protein kinase C (PkcA) suppresses tip dominance in *Dictyostelium discoideum*

Wasima Mohamed [a], Sibnath Ray [b], Derrick Brazill [b], Ramamurthy Baskar [a,*]

[a] Department of Biotechnology, Bhupat and Jyoti Mehta School of Biosciences, Indian Institute of Technology Madras, Chennai 600036, India
[b] Department of Biological Sciences, Center for Translational and Basic Research, Hunter College and The Graduate Center of the City University of New York, New York, NY 10065, USA

ARTICLE INFO

Article history:
Received 11 December 2014
Received in revised form
6 April 2015
Accepted 28 May 2015
Available online 13 July 2015

Keywords:
Dictyostelium
PKC
Morphogenesis
Differentiation
Tip dominance

ABSTRACT

A number of organisms possess several isoforms of protein kinase C but little is known about the significance of any specific isoform during embryogenesis and development. To address this we characterized a PKC ortholog (PkcA; DDB_G0288147) in *Dictyostelium discoideum*. *pkcA* expression switches from prestalk in mound to prespore in slug, indicating a dynamic expression pattern. Mutants lacking the catalytic domain of PkcA (*pkcA*$^-$) did not exhibit tip dominance. A striking phenotype of *pkcA*$^-$ was the formation of an aggregate with a central hollow, and aggregates later fragmented to form small mounds, each becoming a fruiting body. Optical density wave patterns of cAMP in the late aggregates showed several cAMP wave generation centers. We attribute these defects in *pkcA*$^-$ to impaired cAMP signaling, altered cell motility and decreased expression of the cell adhesion molecules – CadA and CsaA. *pkcA*$^-$ slugs showed ectopic expression of *ecmA* in the prespore region. Further, the use of a PKC-specific inhibitor, GF109203X that inhibits the activity of catalytic domain phenocopied *pkcA*$^-$.

1. Introduction

The protein kinase C (PKC) family is a major class of phosphorylating enzymes that catalyse the transfer of a phosphate group from ATP to serine/threonine residues in a protein, thus controlling the protein's functional activity. In mammals, ten different PKC isoforms are known. Depending on their regulatory domains and activators, they are classified as conventional (α, βI, βII, γ), novel (δ, θ, ε, η) or atypical (ζ, λ). For their activation, the conventional isoforms depend on both Ca^{2+} and diacyl glycerol (DAG); the novel isoforms require Ca^{2+} but not DAG, and the atypical isoforms require neither (Steinberg, 2008).

As a group, PKC isoforms play important roles in regulating cell migration, cell proliferation, differentiation and cell death, depending on their cofactors, substrate specificity, tissue distribution and subcellular localization (Mochly-Rosen et al., 2012). During embryonic development, individual PKC isoforms are expressed in distinct patterns (Dehghani and Hahnel, 2005; Eckert et al., 2004). Aberrations in one or more of the PKC isoforms are known to affect cell polarity in *Caenorhabditis elegans* (Tabuse et al., 1998) and to bring about a delay in blastocoel formation in mice (Eckert et al., 2004). In embryonic stem cells, PKC isoforms have been shown to influence lineage specification (Feng et al., 2012) and differentiation (Cho et al., 1998; Dutta et al., 2011; Kindregan et al., 1994) through PKC/ERK1-2, PKC/GSK3β (Kinehara et al., 2013), JNK/c-Jun (Hara et al., 2011), PKC ζ/NF-κB (Rajendran et al., 2013) and Wnt (Liu et al., 2014) signaling pathways. However, isoform-specific PKC knockout (KO) mice did not show any defects during early lineage segregation (Abeliovich et al., 1993; Tan and Parker, 2003). Overall, and as noted in reviews (Basu and Pal, 2010; Chen et al., 2001; Murriel and Mochly-Rosen, 2003), PKCs can exert overlapping, different and even opposite biological functions in the same cell-type, making it difficult at this point to interpret and define the roles of individual isoforms.

To help refine our understanding of the roles of PKCs in development, we employed a simple model organism, *Dictyostelium discoideum* that carries a single isoform of a putative PKC-like protein. *D. discoideum* is a soil-living unicellular eukaryotic amoeba. Growth is characterized by phagocytosis of bacteria, and cells divide by binary fission (Kessin, 2001). When the amoebae are starved, 3′, 5′ cyclic adenosine monophosphate (cAMP) is synthesized and secreted. Alternating pulses of cAMP synthesis and degradation create a relay, leading the amoebae to form a multi-armed, spiraling aggregate, which eventually develops into a migrating slug (McMains et al., 2008). In favorable circumstances, the slug culminates into a fruiting body, comprised of a dead stalk supporting a ball of spores (Kessin, 2001).

In late 1980s, by using effectors like phorbol myristate (PMA)

* Corresponding author.
E-mail address: rbaskar@iitm.ac.in (R. Baskar).

http://dx.doi.org/10.1016/j.ydbio.2015.05.021
0012-1606/

and inhibitors like staurosporine, indirect evidence for the presence of PKC-like activity and its involvement in cAMP receptor regulation during *Dictyostelium* development was reported (Ludérus et al., 1989). Later using crude lysates of *Dictyostelium*, DAG mediated signaling of PKC involved in chemotaxis and development were demonstrated (Phillips et al., 1997). However, due to the lack of genetic evidence, the existence of a true PKC in *Dictyostelium* remains unknown. When the *Dictyostelium* kinome was documented, three different proteins were identified with the classical C1 domain of PKC. These included DDB_G0288147, p-21 activated kinase-D (PAK-D) and ankyrin repeat containing protein (ARCK-1), thus indicating DAG mediated signaling in the organism (Goldberg et al., 2006). Our study shows that DDB_G0288147, which we have called *pkcA*, is a putative PKC ortholog in *D. discoideum*, and has a highly conserved C1 and kinase domain. We find that, as seen in other organisms, the putative PKC is expressed in a cell-type specific manner and is developmentally regulated. The *pkcA* mutant (*pkcA*$^-$) that we engineered to lack the catalytic domain showed impaired early development due to altered cAMP signaling, cell motility and cell–cell adhesion. A striking phenotype of *pkcA*$^-$ was the fragmentation of the aggregates into small territories, each forming a slug and a fruiting body. This result implies that PkcA could be involved in tip dominance.

2. Materials and methods

2.1. Bioinformatics

The FASTA sequence of the putative PKC domain containing protein (DDB_G0288147) was retrieved from dictybase.org (Basu et al., 2013) and used as input for protein architecture analysis by the Simple Modular Architecture Research Tool (SMART) (Schultz et al., 1998). Multiple sequence alignment was carried out by employing Multiple Alignment using Fast Fourier Transform (MAFTT 7) (Katoh and Standley, 2013) and represented using Easy Sequencing in PostScript (ESPript 3) (Robert and Gouet, 2014). A phylogenetic tree was constructed using the neighbor joining method and the BLOSUM 62 scoring matrix of Clustal Ω (Sievers et al., 2011), and represented using FigTree (http://tree.bio.ed.ac.uk/software/figtree/). Protein sequences were retrieved from UniProt (Magrane et al., 2011).

2.2. Strains, cell growth and development

D. discoideum wild type, Ax2, and mutant cells, *pkcA*$^-$, were grown in HL5 liquid medium (14.2 g/l Bacto-peptone, 7.5 g/l yeast extract, 18 g/l maltose, 0.486 g/l KH_2PO_4, 0.506 g/l Na_2HPO_4 supplemented with 100,000 U/l penicillin and 0.1 g/l streptomycin) either as a monolayer in Petri dishes or in flasks as suspension cultures at a cell density of 2–3 $\times 10^6$ cells/ml (Fey et al., 2007). G418 (20 μg/ml) and blasticidin (10 μg/ml) were used for selecting transformants with cell-type specific marker constructs and *pkcA*$^-$ respectively. For development, 4×10^5 cells/cm^2 were spread on 1% non-nutrient agar and allowed to develop in a dark, moist chamber (Fey et al., 2007). For LacZ staining, the samples were fixed in 0.05% glutaraldehyde, permeabilised with 0.1% NP-40 and stained with X-gal solution (5 mM $K_3[Fe(CN)_6]$, 5 mM $K_4[Fe(CN)_6]$, 1 mg/ml 5-bromo-4-chloro 3-indolyl-β-galactoside) (Eichinger and Rivero-Crespo, 2006). Images were captured using a Nikon SMZ1000 stereo zoom microscope.

For generating the *pkcA* promoter construct, a 962 bp regulatory region found upstream of the translation start site was PCR amplified using gDNA as the template and the primers P1 and P2 (Table S1) and ligated in frame with LacZ in pDdGal-16 (Harwood and Drury, 1990) employing the restriction enzymes *Xba*I and *Bgl*II. The engineered *pkcA*-LacZ plasmid was confirmed by PCR and restriction digestion analysis.

For generating the *pkcA* knockout construct, a 2249 bp fragment of the *pkcA* gene, spanning exon 4 was PCR amplified using gDNA as template and the primers, P3 and P4 (Table S1). The amplified DNA was ligated in a TA cloning vector pTZ57R/T (InsTAclone PCR Cloning Kit, Thermo Scientific, USA) to get pMW1. The blasticidin resistance (*bsR*) cassette was excised from pLPBLP vector (Faix et al., 2004) using *Sma*I (New England Biolabs) and *Nde*I (New England Biolabs) and ligated into pMW1 by employing *Nde*I and *Ale*I restriction sites to get *pkcA*-KO.

To express *pkcA* in *pkcA*$^-$ cells, the *pkcA* gene was PCR amplified and placed behind the constitutively active actin 15 promotor to create the plasmid pAct15:*pkcA*. All PCR was performed using the Expand PCR High Fidelity System (Roche, Indianapolis, IN) as per the manufacturer's directions. The *pkcA* gene was amplified using the forward oligonucleotide primer 5′-CACCATGCAACCAAATCAATTAAAAAGAC-3′ and the reverse oligonucleotide primer 5′-TTAATCACAAGCACTGGTATTCTCA-3′. Amplification of the full-length region of *pkcA* was performed on 10 ng genomic DNA with 5 pmol of primers. The resulting PCR product containing the *pkcA* gene was placed behind the constitutively active actin 15 promoter using the Gateway System (Invitrogen, Carlsbad, CA) (Thomason et al., 2006), and transformed into *pkcA*$^-$ cells.

For transformation, 10 μg of the linear *pkcA*-KO fragment and other plasmids were electroporated into Ax2 cells and the positive clones were selected on bacterial lawn/liquid culture containing blasticidin (10 μg/ml) and G418 (20 μg/ml) respectively (Gaudet et al., 2007). Marker constructs for *ecmA*-GFP (Good et al., 2003) and *pspA*-RFP (Parkinson et al., 2009) were kind gifts from Christopher Thompson. p*ecmAO*-LacZ (Parkinson et al., 2009), p*ecmB*-LacZ (Parkinson et al., 2009), p*ecmO*-LacZ (Parkinson et al., 2009) were procured from Dicty Stock Center, USA.

2.3. Isolation of prespore and prestalk specific cell-types

Ax2 cells transformed with *ecmA*-GFP marker construct (Good et al., 2003) were developed on non-nutrient agar for 16 h. Slugs were harvested and mechanically disrupted in KK_2 (2.2 g/l KH_2PO_4, 0.7 g/l K_2HPO_4, pH 6.2) buffer containing 40 mM EDTA (Chen et al., 2004; Kim et al., 2011). Cells dissociated from the slugs were resuspended at a density of 1×10^6 cells/ml and sorted in FACS Aria (BD Biosciences). The isolated cell-types were confirmed by RT-PCR using *pspA* and *ecmA* primers (Table S2).

2.4. Cell–cell adhesion assay

Log phase cells (2–3 $\times 10^6$ cells/ml) were harvested and resuspended at a density of 2×10^7 cells/ml and starved in KK_2 buffer in shaking conditions (175 rpm) at 22 °C for 4 h. The cell suspension was diluted to a density of 2.5×10^6 cells/ml and the aggregates were dispersed by vortexing vigorously for 15 s (Wong et al., 2002). Aggregates were allowed to reform and at indicated time points, the number of non-aggregating cells including singlets and doublets were scored using a Neubauer chamber (Marienfeld, Germany). The total number of aggregates was determined by subtracting the number of singlets/doublets from the total number of cells, which was then expressed as a percentage. To study Ca^{2+} dependent cell–cell adhesion, the assay was performed in the presence of 10 mM EDTA.

2.5. Western blotting

Protein samples were isolated from different developmental stages in sample buffer (62.5 mM Tris–HCl, pH 6.8, 2% SDS, 0.1 M DTT, 10% v/v glycerol) and protein concentration was estimated

using Bradford reagent (BioRad). Equal amounts of protein were loaded in 10% Tris glycine gel (Laemmli, 1970) and after electrophoresis, proteins were transferred onto a nitrocellulose membrane (BioRad). Subsequently, the membrane was blocked with 5% BSA and 0.05% Tween-20 in Tris-buffered saline (TBS) for 1 h at RT. Later, the membrane was incubated overnight at 4 °C with primary antibodies anti-CadA (1:10,000) (Knecht et al., 1987) or anti-CsaA (1:10) (Bertholdt et al., 1985) or anti-actin (1:10) (Simpson et al., 1984). To remove unbound primary antibodies several washes were carried out with TBS–Tween-20, and the membrane was incubated with 1:5000 dilution of HRP conjugated secondary antibody (Bangalore Genei, India) for 1 h at RT. Finally, the membrane was treated with SuperSignal West Pico-chemiluminescent substrate (Thermo Scientific, USA) and the luminescent signals were captured on an X-ray film (GE Amersham, USA). The X-ray film was then developed and scanned. Actin was used as a loading control. Western blotting was carried out thrice and images were quantified using ImageJ (NIH, Bethesda, MD) and normalized to actin expression levels.

2.6. Stalk-cell induction assay

Log phase cells of Ax2/*ecmA*-GFP and *pkcA*$^-$/*ecmA*-GFP were harvested, washed thrice with stalk buffer (10 mM MES, 2 mM NaCl, 10 mM KCl, 1 mM $CaCl_2$, 50 μg/ml streptomycin, 50 U/ml penicillin (pH 6.2)) and incubated in a 24-well plate at 2.5×10^4 cells/cm^2 in stalk buffer supplemented with 5 mM cAMP. After 24 h, cells were washed with stalk buffer to remove cAMP and replaced with the same buffer supplemented with or without differentiation inducing factor-1 (DIF-1) (Good et al., 2003; Kay, 1987). At the end of 24 h incubation, the cells were assayed for prestalk *ecmA* fluorescence and scored for the production of stalk-like cells by phase contrast using an inverted Nikon Eclipse TE2000 microscope.

2.7. cAMP quantification

Log phase *D. discoideum* cells were harvested and plated on 1% non-nutrient agar at a cell density of 5×10^6 cells/cm^2 and were allowed to develop. At the indicated time points, cAMP estimation was carried out using cyclic nucleotide XP Enzymatic ImmunoAssay (EIA) Kit (Cell Signaling Technologies) as per the manufacturer's instructions.

2.8. Semi-quantitative PCR and quantitative reverse transcription PCR

Vegetative *D. discoideum* amoebae were harvested, plated on 1% non-nutrient agar at a density of 5×10^6 cells/cm^2 and at defined time points, RNA was extracted using TRIzol reagent (Life Technologies, USA) (Pilcher et al., 2007). cDNA was synthesized using High Capacity cDNA Reverse Transcription Kit (Applied Biosystems, USA). qPCR for *acaA*, *pde4, 5′nt* and *adk* (Table S2) was carried out with the Eppendorf Real Time PCR platform using DyNAmo Flash SYBR Green qPCR Kit (Thermo Scientific, USA). qPCR was carried out thrice with three biological replicates and analyzed (Schmittgen and Livak, 2008). Semi-quantitative PCR was performed in an Applied Biosystems 2720 Thermocycler using *Taq* polymerase. *rnlA* (Table S2) was used as an internal control and the expression was normalized to the levels of *rnlA*.

2.9. Visualization of cAMP waves

Vegetative cells grown to a density of 2–3 $\times 10^6$ cells/ml were harvested and 5×10^5 cells/cm^2 were plated on 1% non-nutrient agar. The cells were allowed to develop in dark moist condition. The mounds were filmed on a real-time basis at an interval of 10 s/frame for 45 min using a Nikon CCD camera and documented with NIS-Elements D software (Nikon, Japan). For visualizing the optical density waves of cAMP, image pairs (8 frames apart) were subtracted (Siegert and Weijer, 1995) using Image J (NIH, Bethesda, MD). Five different mounds were analyzed on three independent occasions.

2.10. Under-agarose cAMP chemotaxis

The assay was performed according to the established protocol (Woznica and Knecht, 2006) with minor modifications. Vegetative cells were harvested and starved for 1 h at a density of 1×10^7 cells/ml. The cells were pulsed with 30 nM cAMP at 6 min interval for 4 h. Samples of 100 μl of the cell suspension were used for the assay. Cells migrating towards cAMP were recorded every 30 s for 15 min with an inverted Nikon Eclipse TE2000 microscope using NIS-Elements D software (Nikon, Japan). For calculating average velocity, a total of 32 cells from three independent experiments were analyzed. The cells were tracked using ImageJ (NIH, Bethesda, MD).

2.11. F-actin polymerization

TRITC-phalloidin staining of *D. discoideum* cells was used for quantifying F-actin polymerization (Zigmond et al., 1997). Cells were pulsed with 30 nM cAMP at 6 min intervals for 4 h at a density of 1×10^8 cells/ml. After diluting to 1×10^7 cells/ml, the cells were shaken at 200 rpm with 3 mM caffeine for 20 min to synchronize cell signaling. Cells were resuspended in phosphate buffer (10 mM KH_2PO_4, 10 mM K_2HPO_4, pH 6.1, and 2 mM $MgSO_4$) at 3×10^7 cells/ml and stimulated with 100 μM cAMP. 100 μl of cell suspension was taken at 0, 5, 10, 20, 30, 45, 60, 75 and 90 s time points and mixed with actin buffer (20 mM KH_2PO_4, 10 mM PIPES, pH 6.8, 5 mM EGTA, 2 mM $MgCl_2$) containing 4% formaldehyde, 0.1% Triton X-100, and 30 nM TRITC-phalloidin. Cells were stained for 1 h and spun down at 14,000 rpm for 10 min. The pellet was extracted overnight with 1 ml of 100% methanol and the fluorescence was measured (540ex/575em).

2.12. Statistical analyses

Student's *t*-test was performed to calculate statistical significance using Microsoft Excel 2007 and the graphs were plotted using ORIGIN software.

3. Results

3.1. An ortholog of PKC in D. discoideum

To determine whether the PKC domain-containing protein (DDB_G0288147) codes for PKC in *D. discoideum*, the protein sequence was analyzed using the protein architectural analysis tool SMART (Schultz et al., 1998) and aligned with PKCs from other organisms using MAFTT 7 (Katoh and Standley, 2013).

The domain analysis revealed the presence of a C1 domain at the N-terminal region (amino acid residues 13–67) and a C-terminal Ser/Thr kinase domain (amino acid residues 610–851) (Supplementary Fig. 1A). The presence of a single C1 domain with a Ser/Thr kinase domain is a signature of a PKC (Steinberg, 2008). We retrieved the amino acid sequences of all PKC isoforms from UniProt (Magrane et al., 2011) and aligned the C1 and kinase domains using MAFTT 7 (Katoh and Standley, 2013). The C1 domain was identified by the presence of $HX_{12}CX_2CX_NCX_2CX_4HX_2CX_7C$ motif (H is Histidine, C is Cysteine, X is any other amino acid and N

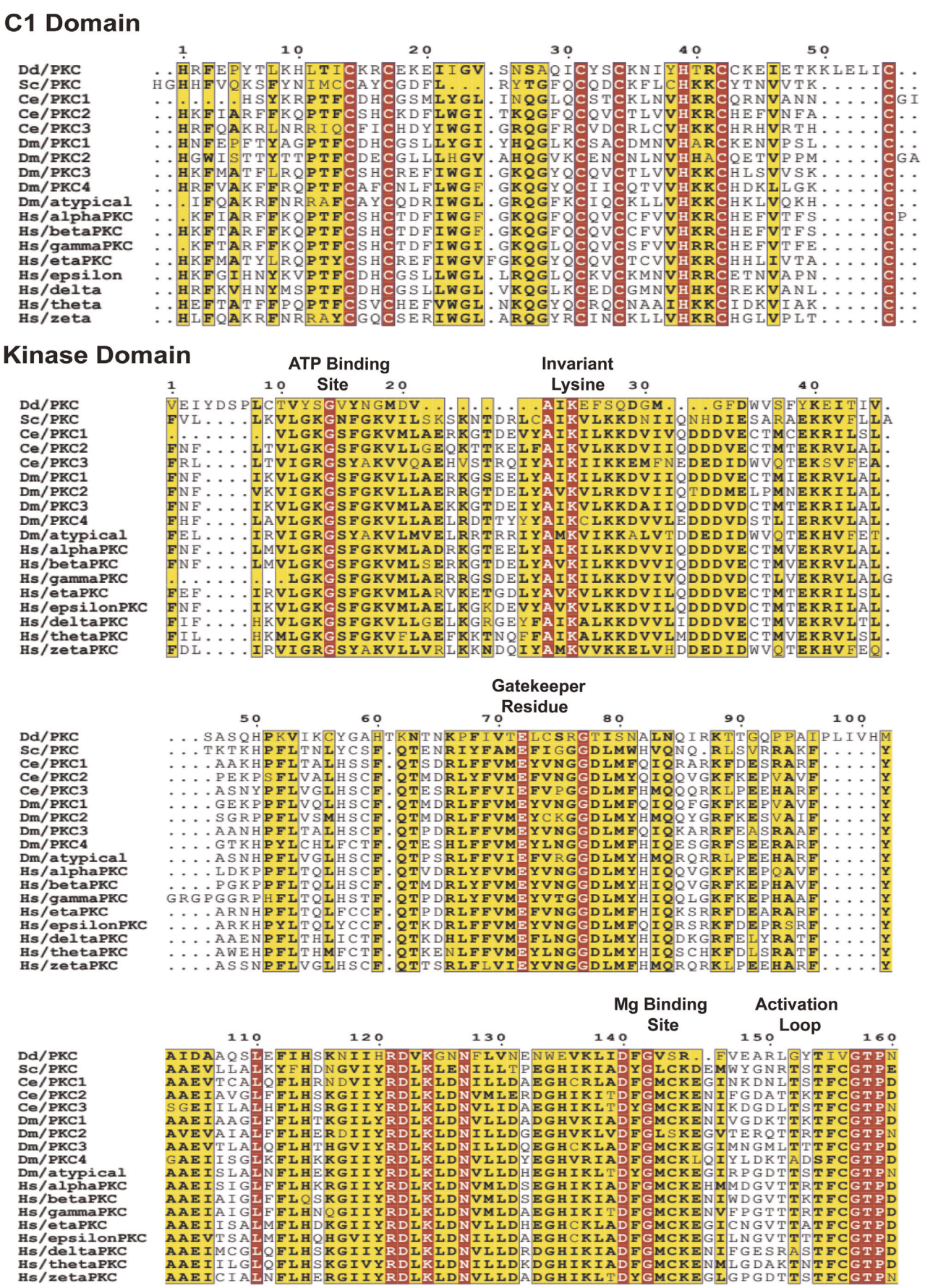

Fig. 1. Conserved C1 and kinase domains of PkcA. Multiple sequence alignment showing conserved residues of PkcA in *D. discoideum* aligned with PKC isoforms of different organisms. Conserved regions are highlighted in yellow and conserved residues in red. C1 domain with aligned cysteine and histidine residues. Kinase domain with aligned ATP binding pocket, invariant lysine, gatekeeper residue, Mg^{2+} binding site and the activation loop.

is 13 or 14). The multiple sequence alignment as represented in Fig. 1 shows that the C1 domain of DDB_G0288147 is highly conserved with an N-terminal region rich in basic residues, suggesting that the protein could be activated by DAG.

A kinase domain in a PKC can be identified by the presence of (a) an invariant lysine that configures the enzyme for phosphoryl-transfer, (b) a gatekeeper methionine residue necessary for restricting flexibility to prevent autocatalytic activation, and (c) a tyrosine residue in the activation loop that consists of a stretch of 20–30 highly conserved amino acid residues (Steinberg, 2008). The activation loop is critical for maintaining the kinase domain in a closed, stabilized, and catalytically competent state by priming/phosphorylating the tyrosine residue (Steinberg, 2008). Interestingly, the multiple sequence alignment indicates K^{626} could act as the invariant lysine. The conserved gate keeper residue role might be played by T^{673} instead of methionine and the stretch of amino acid $DFG^{742–744}$ followed by Y^{756} could form the activation loop (Fig. 1). With these conserved features identified in the PKC domain containing protein (DDB_G0288147), we named the gene encoding this protein as *pkcA*. Further, to understand the relationship between *D. discoideum* PkcA and PKC isoforms from other organisms, we constructed a phylogenetic tree using Clustal Ω (Sievers et al., 2011) which showed that PkcA is most closely related to the atypical and novel PKC isoforms (Supplementary Fig. 1B).

3.2. *pkcA changes from prestalk to prespore expression*

To ascertain whether *pkcA* expression is dynamic in *D. discoideum*, as in other organisms, we monitored its expression by promoter–reporter studies. A *pkcA* promoter construct was generated by ligating the regulatory region of *pkcA* to a construct encoding β-galactosidase (Harwood and Drury, 1990). The accumulation of β-galactosidase was visualized by staining with the substrate X-gal (Fig. 2A). We observed a mosaic expression pattern in the aggregates (8 h) which later was restricted to the aggregate center. By 12 h, *pkcA* expression was restricted to the tipped mound (12 h). At the first finger stage (14 h), the expression increased throughout the elongating tip. Although there is no distinct prestalk and prespore cell-type identity by 8 h of development, it is known that by 12 h, the tip is largely composed of prestalk cells. However, in the slugs, surprisingly, *pkcA* expression was confined to the prespore region (16 h) and continued to be expressed in the prespore region in the culminants (20 h). This sudden shift in *pkcA* expression from the prestalk to the prespore region is suggestive of a dynamic expression pattern. We confirmed prespore-specific expression of *pkcA* in the slugs by semi-quantitative PCR for *pkcA* in prespore and prestalk enriched populations (Fig. 2B). To ensure the purity of the prestalk and prespore enriched populations, primers for *ecmA* and *pspA* were used as controls. In addition, semi-quantitative PCR suggests developmentally regulated expression of *pkcA*, with peaks of expression at 4 h and 16 h of development (Fig. 2C).

3.3. *Aggregates of pkcA⁻ fragment*

pkcA is a single copy gene in *D. discoideum* (Supplementary Fig. 2A) and to understand its role in development, we generated *pkcA⁻* cells by targeted gene disruption of the catalytic domain (Supplementary Fig. 2B). *pkcA⁻* cells were selected using blasticidin, and confirmed by PCR (Supplementary Fig. 2C) using the primer sets P3–P4, P5–P7, P6–P7 (Table S1) and Southern hybridization (Supplementary Fig. 2D). The absence of *pkcA* transcript in *pkcA⁻* cells further confirmed the mutant (Fig. 3A). To examine whether *pkcA⁻* cells showed any developmental defect, we performed a developmental assay with *pkcA⁻* cells. Unlike Ax2, *pkcA⁻* aggregates spiraled around a central hollow within the single multicellular structure, which then fragmented to form multiple mounds (indicated by the arrow in Fig. 3B). The mounds continued to develop into slugs that migrated and formed fruiting bodies resembling those of Ax2 but smaller. When a small molecule inhibitor of the catalytic domain of PKC, GF109203X (Roberts et al., 2004; Toullec et al., 1991), was used, Ax2 aggregates fragmented into multiple mounds, phenocopying the mutant (Fig. 3B). Quantification of this phenotype by counting the number of tipped mounds per unit area formed, showed that *pkcA⁻* cells and Ax2 cells treated with GF109203X formed over twice as many tips as Ax2 cells at 14 h of development (Fig. 3C). This suggests that PkcA kinase activity may be required for tip dominance. Complementation of *pkcA⁻* with pAct15:*pkcA* rescued the developmental defects and the phenotype was comparable

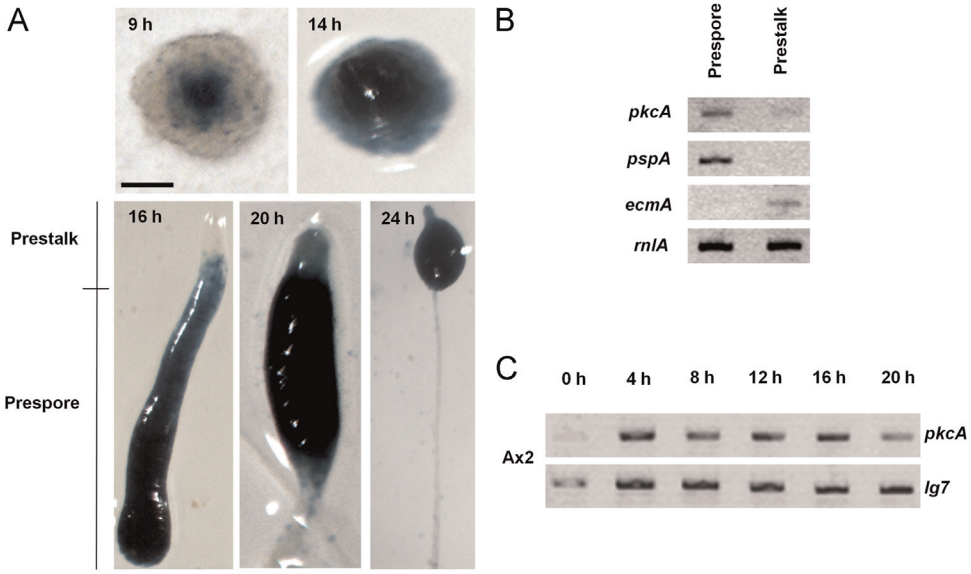

Fig. 2. Dynamic expression pattern of *pkcA*. (A) *pkcA*-LacZ expression at various stages of development. Scale bar—0.2 mm. Semi-quantitative PCR of *pkcA* using RNA extracted from (B) prespore and prestalk enriched cell type, (C) *pkcA* expression throughout development.

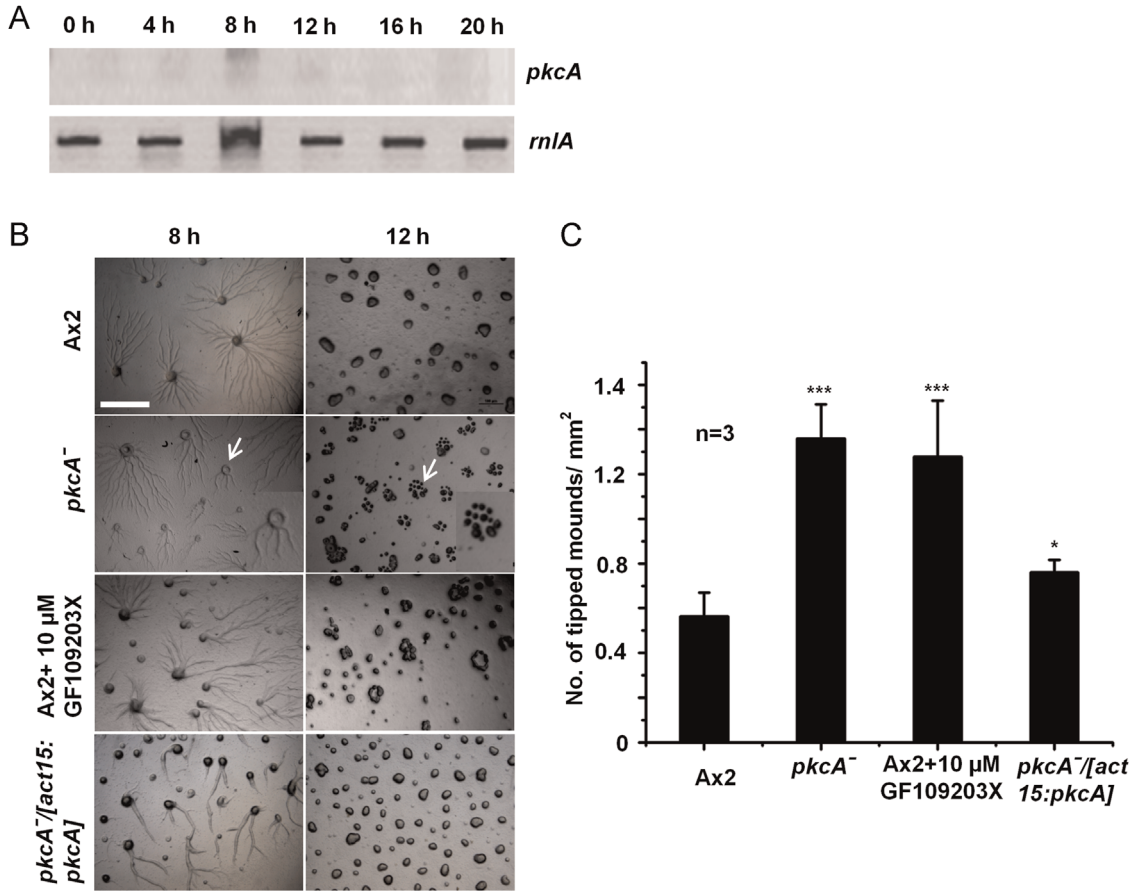

Fig. 3. Fragmenting of late aggregate in *pkcA*$^-$. (A) Absence of *pkcA* expression in *pkcA*$^-$. (B) Developmental profiling of Ax2, *pkcA*$^-$, Ax2 + 10 μM GF109203X and *pkcA*$^-$/[act15:*pkcA*]. Scale bar—0.2 mm. (C) Number of tipped mounds formed per unit area by 14 h of development of Ax2, *pkcA*$^-$, Ax2 + 10 μM GF109203X and *pkcA*$^-$/[act15:*pkcA*], represented as a bar graph; error bars show the standard deviation. The number of tipped mounds was quantified from ten different frames. Three independent experiments in triplicate were carried out. Level of significance is indicated as $^*p < 0.05$, $^{**}p < 0.01$, $^{***}p < 0.001$, and $^{****}p < 0.0001$.

to Ax2 (Fig. 3B and C).

3.4. *pkcA*$^-$ late aggregates displayed multiple cAMP wave generating centers

The periodic synthesis and secretion of cAMP by cells in the aggregation center directs further development in *D. discoideum*. Detection and amplification of these signals by the surrounding cells, coupled with desensitization of the cAMP producing cells, results in outward propagation of cAMP waves from the aggregation center (Weijer, 2004). cAMP waves guide the cells to move towards a common center and form a mound. The propagating waves can be observed by the differences in the optical density of cells moving in response to cAMP waves. To determine whether the breaking up of late aggregates of *pkcA*$^-$ cells is due to the loss of a dominant signaling center, we visualized cAMP waves by recording development in real time, and then subtracted the image pairs that were 8 frames apart (Siegert and Weijer, 1995). Unlike Ax2, which had a single wave generating center with spiraling arms moving in the outward direction, *pkcA*$^-$ and Ax2 cells developed in the presence of the inhibitor GF109203X had several wave propagating centers (Fig. 4A, Supplementary Videos S1–S3). Each wave propagating center fragmented and progressed to form independent fruiting bodies. The optical density analysis clearly suggests that cAMP wave generation in *pkcA*$^-$ cells is defective. Like Ax2, the complemented strain, *pkcA*$^-$/[act15:*pkcA*] had a single cAMP wave generating center (Fig. 4A and Supplementary Video S4).

Supplementary material related to this article can be found online at doi:10.1016/j.ydbio.2015.05.021.

3.5. *pkcA*$^-$ cells are impaired in cAMP relay

The key players involved in cAMP relay are adenylate cyclase A (ACA), which synthesizes cAMP, and cAMP phosphodiesterases (PDEs), which degrade cAMP to AMP (Saran et al., 2002). The degradation of cAMP is further driven by the relative levels of 5′ nucleotidase (5′NT) and adenosine kinase (ADK), which catalyse the conversion of AMP to adenosine (Wiles, 2005). To investigate whether the regulation of genes involved in cAMP relay is disturbed, we determined the expression levels of these genes at 9 h and 12 h of development by qRT-PCR (Fig. 4B). Although there was no change in the *acaA* expression at either 9 h or 12 h, the expression levels of *pde4, 5′nt* and *adk* were reduced. There was no significant change in *pde4* expression at 9 h but a decrease in expression was observed by 12 h. There was a significant decrease in *5′nt* and *adk* expression at 9 h and 12 h. To ascertain whether the downregulation of genes involved in cAMP degradation in *pkcA*$^-$ cells affected cAMP levels, total intracellular and extracellular cAMP levels at 9 h and 12 h of development were quantified. We observed a significant increase in cAMP levels by 9 h and 12 h, in *pkcA*$^-$ cells compared to Ax2 (Fig. 4C). This suggests that the decreased expression of *5′nt* and *adk* may manifest as an increased level of cAMP.

3.6. *pkcA*$^-$ is defective in chemotaxis and cell–cell adhesion

In addition to the influence of the cAMP relay, the integrity of

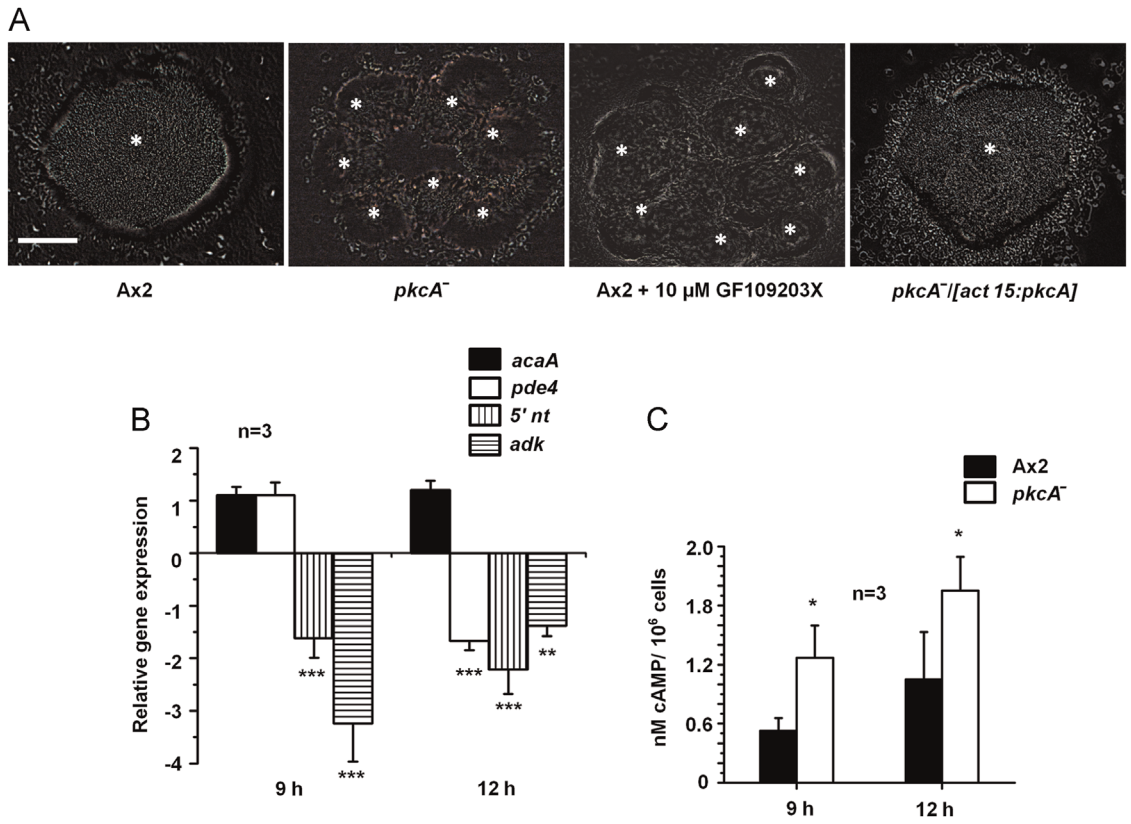

Fig. 4. *pkcA*$^-$ is defective in cAMP relay. (A) cAMP wave generating centers are represented by optical density waves. Wave generating centers are indicated by asterixes. Scale bar—0.2 mm. (B) Bar graph representing the relative change in the expression levels of *acaA*, *pde4*, *5′nt* and *adk* of *pkcA*$^-$ in comparison to Ax2 at 9 h and 12 h of development. (C) cAMP levels of Ax2 and *pkcA*$^-$ at 9 h and 12 h of development. The experiments were carried out thrice; mean and standard deviation are represented as error bars. Level of significance is indicated as $^*p < 0.05$, $^{**}p < 0.01$, $^{***}p < 0.001$, and $^{****}p < 0.0001$.

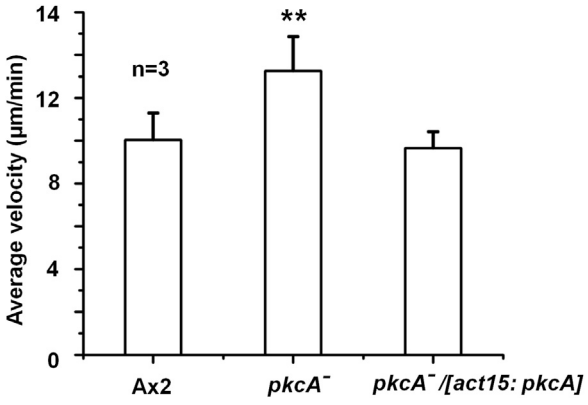

Fig. 5. cAMP chemotaxis. Average chemotactic velocity of Ax2, *pkcA*$^-$ and *pkcA*$^-$/[act15:*pkcA*] in response to cAMP; error bars show the standard deviation. Velocity is calculated by dividing the total displacement of the cells by time. A total of 32 cells from three independent experiments was used to calculate the average velocity. Level of significance is indicated as $^*p < 0.05$, $^{**}p < 0.01$, $^{***}p < 0.001$, and $^{****}p < 0.0001$.

the aggregates is governed by two other major factors: (a) chemotaxis towards cAMP and (b) cell–cell adhesion (Gomer et al., 2011; Jang and Gomer, 2008; Pálsson et al., 1997). To measure cell movement in response to a cAMP gradient, we performed an under-agarose cAMP chemotaxis assay (Woznica and Knecht, 2006). For this assay, Ax2 and *pkcA*$^-$ cells were allowed to starve on a shaker with pulsing of 30 nM cAMP. This mimics early developmental signaling, making the cells competent for chemotaxis towards cAMP (McMains et al., 2008). Cell movement towards cAMP was recorded for 15 min at 30 s intervals, and the average velocity (total displacement divided by time) was calculated. In agreement with earlier reports, the velocity of Ax2 cells was 10.04 ± 1.24 μm/min (Chen and Segall, 2006; Plak et al., 2013; Veltman et al., 2008), and interestingly, that of *pkcA*$^-$ cells was 13% higher (Fig. 5) The chemotaxis defects of *pkcA*$^-$ was restored in the complemented strain *pkcA*$^-$/[act15:*pkcA*] with responses similar to Ax2.

Changes in cell motility are typically associated with changes in the actin cytoskeleton. Hence, we tested the *in vivo* polymerization of F-actin in response to cAMP stimulation (Zigmond et al., 1997). *In vivo* F-actin polymerization studies were carried out by stimulating starved cells with cAMP, followed by fixing and staining the cells with TRITC-phalloidin at different time points. As reported earlier, after 10 s exposure to cAMP, the characteristic increase in F-actin polymerization was observed in Ax2 (Chung et al., 2000; Myers et al., 2005) while in *pkcA*$^-$ cells the increase was about twice that of Ax2 cells (Fig. 6). Microscopic examination of cell shape during chemotaxis showed that *pkcA*$^-$ cells often produced bifurcating pseudopods with a deep curvature at the front end (not shown), consistent with there being increased F-actin polymerization in *pkcA*$^-$ cells. Similar observation of increased F-actin polymerization has been observed in *pirA*$^-$ strain that leads to the splitting of the front-end pseudopods (Blagg et al., 2003). This suggests that PkcA could be involved in inhibiting F-actin polymerization and thus pseudopod formation during cAMP chemotaxis.

Next, the cell–cell adhesion properties of *pkcA*$^-$ cells were examined. Developing amoebae express two major cell–cell adhesion proteins, CadA, expressed 2 h post-starvation, and CsaA expressed during early aggregation (6 h). CadA-mediated cell–cell adhesion is Ca^{2+}-dependent and is thus EDTA-sensitive, while

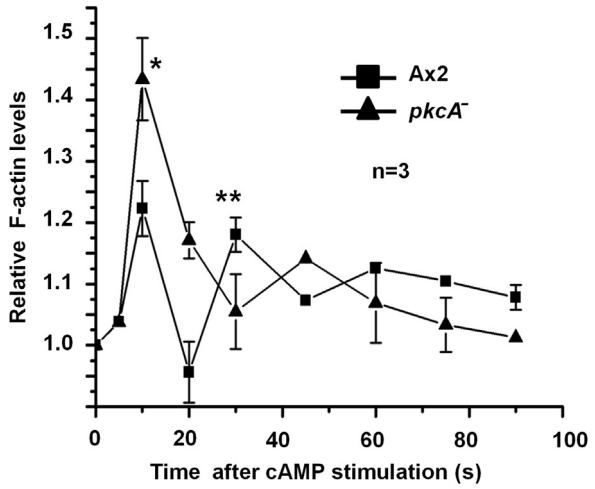

Fig. 6. Actin polymerization. *In vivo* actin polymerization assay measuring F-actin levels in response to cAMP stimulation. After 10 s exposure to cAMP, actin polymerization in *pkcA*$^-$ increased two-fold compared to Ax2 cells. Level of significance is indicated as $^*p < 0.05$, $^{**}p < 0.01$, $^{***}p < 0.001$, and $^{****}p < 0.0001$. The experiment was carried out thrice with two biological replicates.

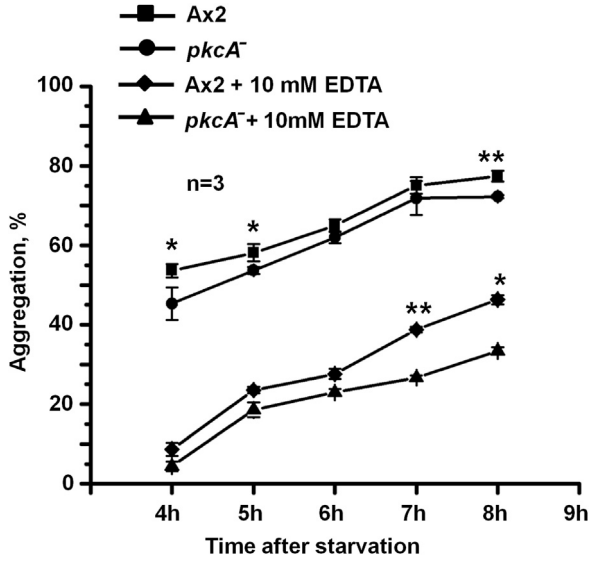

Fig. 7. Cell adhesion properties of *pkcA*$^-$.Cell–cell adhesion profiles of starved Ax2 and *pkcA*$^-$ cells shaken in suspension. The assay was carried out thrice with three biological replicates both in the presence and absence of 10 mM EDTA. Mean values of percent aggregation; error bars show the standard deviation.

CsaA is Ca^{2+}-independent and EDTA-resistant (Coates and Harwood, 2001). The adhesive properties of Ax2 and *pkcA*$^-$ cells were measured after allowing the cells to develop for 4 h in suspension and then mechanically dispersing clumps into single cells. Cells were then allowed to aggregate again in the presence or absence of 10 mM EDTA, and the numbers of singlets and doublets were counted (Fig. 7). *pkcA*$^-$ cells showed reduced cell–cell adhesion both in the presence of chelators (5–15%) and in their absence (20–50%) suggesting that cAMP induced expression of both CadA and CsaA is reduced. This reduction in expression was confirmed by Western blot analysis of CadA and CsaA (Supplementary Fig. 3A and B). Taken together, these results indicate the disruption, in *pkcA*$^-$ cells, of two processes required for aggregate integrity, namely chemotaxis towards cAMP and cell–cell adhesion.

3.7. *pkcA*$^-$ cells possess cell autonomous and non-autonomous defects

D. discoideum morphogenesis is a result of the co-ordinated chemotactic movement of the developing cells and the signaling mediated by cell–cell contact (Weijer, 2004). Any defect in these processes could affect differentiation and sorting during multicellular development. To examine whether there were defects in sorting of the cell-types in *pkcA*$^-$ slugs, we transformed Ax2 and *pkcA*$^-$ cells with prestalk (*ecmA*, *ecmO*, *ecmAO* and *ecmB*) and prespore (*pspA*) cell-type specific markers and monitored their expression at the slug stage (16 h). *pkcA*$^-$ and Ax2 slugs showed the same expression patterns for the prespore marker (*pspA*) and one of the prestalk markers (*ecmB*) (Supplementary Fig. 4A and B). However, in *pkcA*$^-$ slugs the prestalk marker *ecmA* was observed not only in the prestalk region but also at a lower level in the prespore region while in Ax2 slugs it was confined exclusively to the prestalk region of the slug anterior (Fig. 8A). Similarly, the expression patterns of the other prestalk markers (*ecmO* and *ecmAO*) in *pkcA*$^-$ slugs differed from those in Ax2 slugs (Supplementary Fig. 4C and D). In addition, *pkcA*$^-$ showed early expression of *ecmA* as observed by semi-quantitative PCR performed with RNA isolated from different stages of development. In *pkcA*$^-$ cells, *ecmA* expression started as early as 10 h of development, compared to Ax2 cells, which began expression at 12 h of development (Fig. 8B). This suggests that *pkcA*$^-$ is defective in regulating the temporal and spatial expression of prestalk genes.

These differentiation defects in *pkcA*$^-$ could either be due to faults in producing the signal (cell non-autonomous) or could be an intracellular defect in perceiving or processing the signal by the differentiating cell (cell autonomous). To differentiate between the cell autonomous and non-autonomous roles of PkcA in development, chimeras of Ax2 and *pkcA*$^-$ cells were created at different

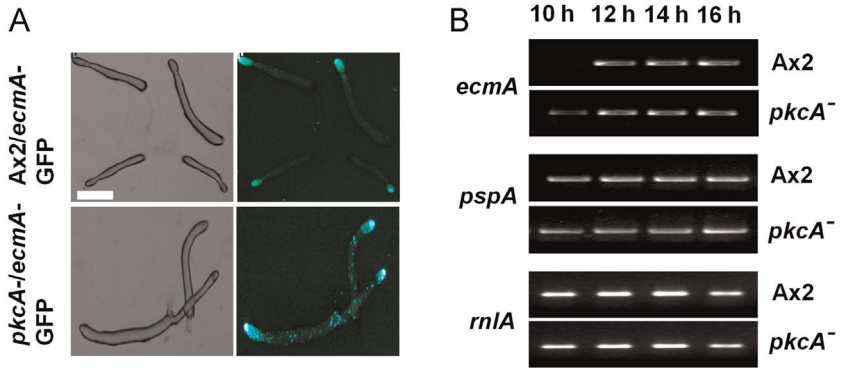

Fig. 8. Defective *ecmA* expression in *pkcA*$^-$. (A) *ecmA*-GFP expression in Ax2 and *pkcA*$^-$ cells at 16 h of development. Scale bar—0.5 mm. (B) Semi-quantitative PCR for *ecmA* and *pspA* of RNA isolated from Ax2 and *pkcA*$^-$ at 10 h, 12 h, 14 h and 16 h of development.

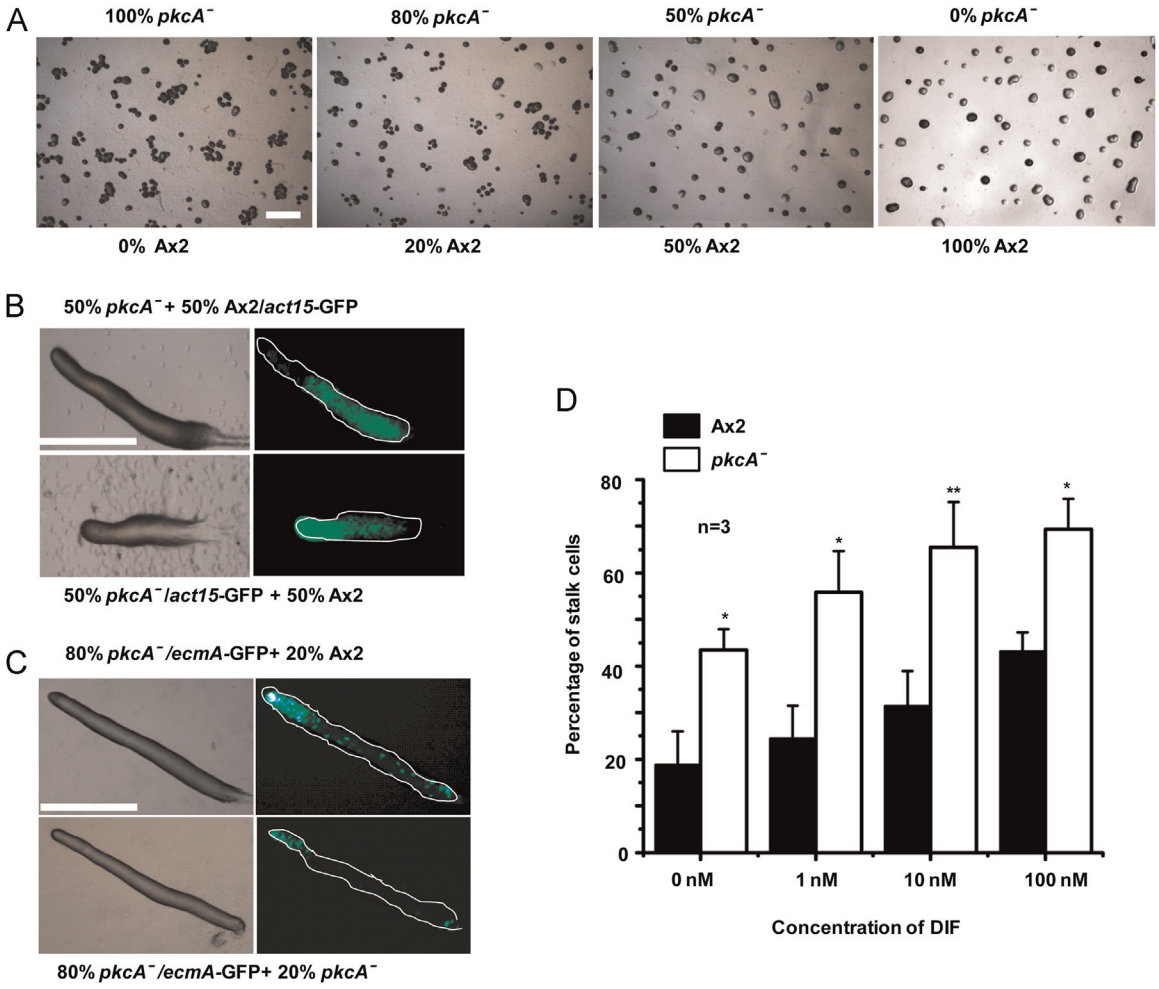

Fig. 9. Cell autonomous and non-autonomous defects in *pkcA*$^-$. (A) Reconstitution of *pkcA*$^-$ with Ax2 cells in different ratios reduced the fragmentation defects of *pkcA*$^-$ aggregates. (B) 50% unlabeled *pkcA*$^-$, when reconstituted with 50% labeled Ax2 expressing *act15*-GFP and vice-versa show a prestalk cell fate bias. (C) Reconstitution of 20% labeled *pkcA*$^-$ expressing *ecmA*-GFP with 80% unlabeled Ax2 cells show cell autonomous prestalk differentiation defect. Scale bar—1.0 mm. (D) Stalk cell induction assay performed with Ax2 and *pkcA*$^-$ cells expressing *ecmA*-GFP in the presence of 0 nM, 1 nM, 10 nM, and 100 nM of DIF. Mean values of three independent experiments in triplicate; error bars show the standard deviation. Level of significance is indicated as * $p < 0.05$, ** $p < 0.01$, *** $p < 0.001$, and **** $p < 0.0001$.

ratios. Remarkably, tip dominance was partially rescued when *pkcA*$^-$ cells were co-developed with 50% Ax2 (Fig. 9A). In chimeras with 50% unlabeled *pkcA*$^-$ and 50% *act-15*/GFP expressing Ax2 cells, the unlabeled *pkcA*$^-$ preferentially populate the anterior prestalk region of the slug (Fig. 9B). When 20% *pkcA*$^-$ marked with *ecmA*/GFP were reconstituted with 80% unlabeled Ax2 cells, *pkcA*$^-$ were unable to restrict *ecmA*/GFP expression to the prestalk as the scattered expression could be seen even in the prespore region (Fig. 9C).

To further examine the cell autonomous nature of the differentiation defect of the *pkcA*$^-$ cells, terminal differentiation under monolayer conditions (Good et al., 2003; Kay, 1987) was carried out. Stalk cell differentiation was induced by sequential exposure of cells to cAMP and varying concentrations of DIF-1 (Good et al., 2003; Harwood et al., 1995; Wang and Kuspa, 2002). Under these conditions, 45–65% of *pkcA*$^-$/*ecmA*-GFP cells formed vacuolated stalk cells in the presence of DIF. In contrast, only 20–40% Ax2/*ecmA*-GFP cells became vacuolated and formed stalk cells. A 1.5–2.5 fold increase in stalk cell formation was observed in *pkcA*$^-$/*ecmA*-GFP with increasing concentrations of DIF (Fig. 9D).

4. Discussion

Phosphatases and kinases control the active and inactive states of a number of proteins involved in signaling. One such transducer is PKC, ubiquitously present in organisms from yeast to metazoans, but absent in plants (Goldberg et al., 2006). The number of PKC isoforms in any given organism varies from one to 10. Yeasts have a single copy of PKC-like protein; nematodes have three isoforms, fruit flies have five, and mammals 10. It is interesting that a lower eukaryote such as *D. discoideum* encodes a protein with highly conserved PKC C1 and kinase domains (Fig.1). Being a large family with overlapping substrates, it is a challenge to assign specific roles to each PKC isoform. Here, we report the characterization of the *pkcA*, that it is involved in cAMP relay and cell-type differentiation.

pkcA$^-$ cells had severe aggregation defects, with aggregates fragmenting into several mounds (Fig. 3B). The ability of cells to form stable, appropriately sized aggregates depends upon cAMP relay, chemotaxis, cytoskeletal dynamics and cell–cell adhesion (McMains et al., 2008). It is reported that when the equilibrium between chemotaxis and cell–cell adhesion factors is disturbed, streams break and reorganize themselves to form individual mounds (Jang and Gomer, 2008). We see that *pkcA*$^-$ cells have enhanced chemotactic speed and decreased cell–cell adhesion, most likely due to increased F-actin polymerization and reduced expression of adhesion molecules, respectively. Our experiments thus suggest that the loss of integrity in *pkcA*$^-$ aggregates may be due to defects in chemotaxis towards cAMP and reduced cell–cell

adhesion.

As demonstrated by qPCR, *pkcA*$^-$ had altered expression of cAMP relay genes-*pde4*, 5′*nt* and *adk*. This differential expression could manifest in altered cAMP levels in *pkcA*$^-$. cAMP quantification indeed suggests increased cAMP levels at 9 h and 12 h of development. The strength of cAMP relay is one of the factors that regulate aggregate size (Jang and Gomer, 2008). For example, *cnrN*$^-$ cells have excess cAMP that leads to reduced aggregate territory size (Tang and Gomer, 2008). Late aggregates of *pkcA*$^-$ had several cAMP signaling centers suggesting a significant role of PkcA in cAMP relay during development.

In addition to their morphogenetic defects, *pkcA*$^-$ cells exhibit differentiation defects. *pkcA*$^-$ cells preferentially differentiated into stalk cells in a stalk cell differentiation assay. Moreover, *pkcA*$^-$ cells preferentially sorted to the prestalk regions of chimeric slugs, demonstrating that this is a cell autonomous effect. The reason for this may be found in the aberrant temporal and spatial expression of prestalk genes observed in *pkcA*$^-$ cells. *pkcA*$^-$ cells express *ecmA* earlier in development than the wildtype. In addition, the expression of *ecmA*, *ecmO* and *ecmAO* is not properly localized in *pkcA*$^-$ slugs (Fig. 8A and Supplementary Fig. 4C and D). The mislocalization of *ecmA* expression is not rescued by mixing with Ax2 cells (Fig. 9C), reinforcing the suggestion that this is a cell autonomous defect. The patterning defects of *ecmA*, *ecmAO*, *ecmO* in *pkcA*$^-$ and the increased prestalk cell type differentiation in monolayer conditions (Fig. 9D), suggest that PkcA could be involved in transcriptional regulation of prestalk patterning (Williams, 2006).

Interestingly, the cell differentiation defect seen in *pkcA*$^-$ cells may originate during tip formation. Little is known about the mechanism of cell fate decisions involved in tip development. However, the observed pattern of *pkcA* expression may provide some insight; *pkcA* is expressed throughout development and switches from the prestalk region (tip) in late aggregates, to the prespore region (posterior) in the slug.

Many of the defects associated with loss of PkcA can be phenocopied by the treatment of Ax2 cells with 10 μM GF109203X, a small molecule inhibitor known to block the catalytic domain of PKC. This is consistent with the kinase activity being crucial for PkcA function in these processes. In mammalian systems, PKCs phosphorylate a number of proteins, such as extracellular receptor kinase-1/2 (ERK1/2), glycogen synthase 3β (GSK3β) (Rosse et al., 2010), nuclear factor kappa-light-chain-enhancer of activated B cells (NFκβ) (Dutta et al., 2011), and regulate cellular processes such as developmental cell-fate specification, differentiation (Dutta et al., 2011), establishment of cell–cell contact during embryo compaction (Pauken and Capco, 1999), cell polarity (Tabuse et al., 1998) and cell migration (Rosse et al., 2010).

5. Conclusion

We report the characterization of *pkcA* in *Dictyostelium. pkcA* is expressed throughout development and switches from prestalk in late aggregates to prespore in the slugs. Our experiments demonstrate the role of PkcA in development and cell-type differentiation. The use of PKC specific inhibitor, GF109203X that inhibits the activity of catalytic domain manifests in a phenotype similar to the loss of *pkcA* supporting that *pkcA* could possibly code for a PKC ortholog.

Conflict of interest

All the authors declare that no competing interests exist.

Authors contributions

WM and RB conceived and designed the experiments. WM performed and analyzed all the experiments. SR and DB generated the *pkcA* expression construct. WM wrote the manuscript and RB, DB edited the manuscript.

Acknowledgments

We thank Chi-Sui, Angelika Noegel and Ludwig Eichinger for providing the antibodies used in this work. Authors thank the Indian Institute of Technology Madras, the Council of Scientific and Industrial Research, New Delhi, India and the Department of Science and Technology, Ministry of Science and Technology, New Delhi, India for financial support. WM gratefully acknowledges the technical support from Jasmine M. Shah, Shashi Prakash Singh, Amit Kumar Singh, Debanjan Tewari, Prashant Kumar, Chellam Gayathri, Mrithyunjay and Nasna Nassir. We acknowledge Dr. Ranjani Dhakshinamoorthy, Shalini U. and Malini Sundar Rajan for editing the manuscript.

Appendix A. Supplementary information

Supplementary data associated with this article can be found in the online version at http://dx.doi.org/10.1016/j.ydbio.2015.05.021.

References

Abeliovich, A., Chen, C., Goda, Y., Silva, A.J., Stevens, C.F., Tonegawa, S., 1993. Modified hippocampal long-term potentiation in PKCγ-mutant mice. Cell 75, 1253–1262.
Basu, A., Pal, D., 2010. Two faces of protein kinase Cδ: the contrasting roles of PKCδ in cell survival and cell death. Sci. World J. 10, 2272–2284.
Basu, S., Fey, P., Pandit, Y., Dodson, R., Kibbe, W.A., Chisholm, R.L., 2013. DictyBase 2013: integrating multiple Dictyostelid species. Nucl. Acids Res. 41, D676–D683.
Bertholdt, G., Stadler, J., Bozzaro, S., Fichtner, B., Gerisch, G., 1985. Carbohydrate and other epitopes of contact site A glycoprotein of *Dictyostelium discoideum* as characterized by monoclonal antibodies. Cell Differ. 16, 187–202.
Blagg, S.L., Stewart, M., Sambles, C., Insall, R.H., 2003. PIR121 regulates pseudopod dynamics and SCAR activity in Dictyostelium. Curr. Biol. 13, 1480–1487.
Chen, G., Shaulsky, G., Kuspa, A., 2004. Tissue-specific G1-phase cell-cycle arrest prior to terminal differentiation in Dictyostelium. Development 131, 2619–2630.
Chen, L., Hahn, H., Wu, G., Chen, C.-H., Liron, T., Schechtman, D., Cavallaro, G., Banci, L., Guo, Y., Bolli, R., 2001. Opposing cardioprotective actions and parallel hypertrophic effects of δPKC and εPKC. Proc. Natl. Acad. Sci. 98, 11114–11119.
Chen, S., Segall, J.E., 2006. EppA, a putative substrate of DdERK2, regulates cyclic AMP relay and chemotaxis in *Dictyostelium discoideum*. Eukaryot. Cell 5, 1136–1146.
Cho, Y., Klein, M.G., Talmage, D.A., 1998. Distinct functions of protein kinase Calpha and protein kinase Cbeta during retinoic acid-induced differentiation of F9 cells. Cell Growth Differ.: Mol. Biol. J. Am. Assoc. Cancer Res. 9, 147–154.
Chung, C.Y., Lee, S., Briscoe, C., Ellsworth, C., Firtel, R.A., 2000. Role of Rac in controlling the actin cytoskeleton and chemotaxis in motile cells. Proc. Natl. Acad. Sci. 97, 5225–5230.
Coates, J.C., Harwood, A.J., 2001. Cell–cell adhesion and signal transduction during Dictyostelium development. J. Cell Sci. 114, 4349–4358.
Dehghani, H., Hahnel, A.C., 2005. Expression profile of protein kinase C isozymes in preimplantation mouse development. Reproduction 130, 441–451.
Dutta, D., Ray, S., Home, P., Larson, M., Wolfe, M.W., Paul, S., 2011. Self-renewal versus lineage commitment of embryonic stem cells: protein kinase C signaling shifts the balance. Stem Cells 29, 618–628.
Eckert, J.J., McCallum, A., Mears, A., Rumsby, M.G., Cameron, I.T., Fleming, T.P., 2004. Specific PKC isoforms regulate blastocoel formation during mouse preimplantation development. Dev. Biol. 274, 384–401.
Eichinger, L., Rivero-Crespo, F., 2006. *Dictyostelium discoideum* Protocols. Springer.
Faix, J., Kreppel, L., Shaulsky, G., Schleicher, M., Kimmel, A.R., 2004. A rapid and efficient method to generate multiple gene disruptions in *Dictyostelium discoideum* using a single selectable marker and the Cre-loxP system. Nucl. Acids Res. 32, e143-e143.
Feng, X., Zhang, J., Smuga-Otto, K., Tian, S., Yu, J., Stewart, R., Thomson, J.A., 2012. Protein kinase C mediated extraembryonic endoderm differentiation of human embryonic stem cells. Stem Cells 30; , pp. 461–470.

Fey, P., Kowal, A.S., Gaudet, P., Pilcher, K.E., Chisholm, R.L., 2007. Protocols for growth and development of *Dictyostelium discoideum*. Nat. Protoc. 2, 1307–1316.
Gaudet, P., Pilcher, K.E., Fey, P., Chisholm, R.L., 2007. Transformation of *Dictyostelium discoideum* with plasmid DNA. Nat. Protoc. 2, 1317–1324.
Goldberg, J.M., Manning, G., Liu, A., Fey, P., Pilcher, K.E., Xu, Y., Smith, J.L., 2006. The dictyostelium kinome—analysis of the protein kinases from a simple model organism. PLoS Genet. 2, e38.
Gomer, R.H., Jang, W., Brazill, D., 2011. Cell density sensing and size determination. Dev., Growth Differ. 53, 482–494.
Good, J.R., Cabral, M., Sharma, S., Yang, J., Van Driessche, N., Shaw, C.A., Shaulsky, G., Kuspa, A., 2003. TagA, a putative serine protease/ABC transporter of Dictyostelium that is required for cell fate determination at the onset of development. Development 130, 2953–2965.
Hara, T., Miyazaki, M., Hakuno, F., Takahashi, S., Chida, K., 2011. PKCη promotes a proliferation to differentiation switch in keratinocytes via upregulation of p27Kip1 mRNA through suppression of JNK/c-Jun signaling under stress conditions. Cell Death Dis. 2, e157.
Harwood, A., Drury, L., 1990. New vectors for expression of the *E. coli* lacZ gene in Dictyostelium. Nucl. Acids Res. 18, 4292.
Harwood, A., Plyte, S., Woodgett, J., Strutt, H., Kay, R., 1995. Glycogen synthase kinase 3 regulates cell fate in Dictyostelium. Cell 80, 139–148.
Jang, W., Gomer, R.H., 2008. Combining experiments and modelling to understand size regulation in *Dictyostelium discoideum*. J. R. Soc. Interface 5, S49–S58.
Katoh, K., Standley, D.M., 2013. MAFFT multiple sequence alignment software version 7: improvements in performance and usability. Mol. Biol. Evol. 30, 772–780.
R.R. Kay, 1987. Cell differentiation in monolayers and the investigation of slime mold morphogens. In: Spudich, J.A. (Ed.), Methods in Cell Biology *Dictyostelium discoideum*: Molecular Approaches to Cell Biology, vol. 28. p. 433.
Kessin, R.H., 2001. Dictyostelium: Evolution, Cell Biology, and the Development of Multicellularity. Cambridge University Press, Cambridge.
Kim, L., Brzostowski, J., Majithia, A., Lee, N.-S., McMains, V., Kimmel, A.R., 2011. Combinatorial cell-specific regulation of GSK3 directs cell differentiation and polarity in Dictyostelium. Development 138, 421–430.
Kindregan, H.C., Rosenbaum, S.E., Ohno, S., Niles, R.M., 1994. Characterization of conventional protein kinase C (PKC) isotype expression during F9 teratocarcinoma differentiation. Overexpression of PKC alpha alters the expression of some differentiation-dependent genes. J. Biol. Chem. 269, 27756–27761.
Kinehara, M., Kawamura, S., Tateyama, D., Suga, M., Matsumura, H., Mimura, S., Hirayama, N., Hirata, M., Uchio-Yamada, K., Kohara, A., 2013. Protein kinase C regulates human pluripotent stem cell self-renewal. PloS One 8, e54122.
Knecht, D.A., Fuller, D.L., Loomis, W.F., 1987. Surface glycoprotein, gp24, involved in early adhesion of *Dictyostelium discoideum*. Dev. Biol. 121, 277–283.
Laemmli, U.K., 1970. Cleavage of structural proteins during the assembly of the head of bacteriophage T4. Nature 227, 680–685.
Liu, A., Chen, S., Cai, S., Dong, L., Liu, L., Yang, Y., Guo, F., Lu, X., He, H., Chen, Q., 2014. Wnt5a through noncanonical Wnt/JNK or Wnt/PKC signaling contributes to the differentiation of mesenchymal stem cells into type II alveolar epithelial cells in vitro. PloS One 9, e90229.
Ludérus, M., Van der Most, R.G., Otte, A.P., Van Driel, R., 1989. A protein kinase C-related enzyme activity in *Dictyostelium discoideum*. FEBS Lett. 253, 71–75.
Magrane, M., Consortium, U., 2011. UniProt Knowledgebase: a hub of integrated protein data. Database 2011, bar009.
McMains, V.C., Liao, X.-H., Kimmel, A.R., 2008. Oscillatory signaling and network responses during the development of *Dictyostelium discoideum*. Ageing Res. Rev. 7, 234–248.
Mochly-Rosen, D., Das, K., Grimes, K.V., 2012. Protein kinase C, an elusive therapeutic target? Nat. Rev. Drug Discov. 11, 937–957.
Murriel, C.L., Mochly-Rosen, D., 2003. Opposing roles of δ and ε PKC in cardiac ischemia and reperfusion: targeting the apoptotic machinery. Arch. Biochem. Biophys. 420, 246–254.
Myers, S.A., Han, J.W., Lee, Y., Firtel, R.A., Chung, C.Y., 2005. A Dictyostelium homologue of WASP is required for polarized F-actin assembly during chemotaxis. Mol. Biolo. Cell 16, 2191–2206.
Pálsson, E., Lee, K.J., Goldstein, R.E., Franke, J., Kessin, R.H., Cox, E.C., 1997. Selection for spiral waves in the social amoebae Dictyostelium. Proc. Natl. Acad. Sci. 94, 13719–13723.
Parkinson, K., Bolourani, P., Traynor, D., Aldren, N.L., Kay, R.R., Weeks, G., Thompson, C.R., 2009. Regulation of Rap1 activity is required for differential adhesion, cell-type patterning and morphogenesis in Dictyostelium. J. Cell Sci. 122, 335–344.
Pauken, C.M., Capco, D.G., 1999. Regulation of cell adhesion during embryonic compaction of mammalian embryos: Roles for PKC and β-catenin. Mol. Reprod. Dev. 54, 135–144.
Phillips, P., Thio, M., Pears, C., 1997. A protein kinase C-like activity involved in the chemotactic response of *Dictyostelium discoideum*. Biochim. Biophys. Acta (BBA)—Lipids Lipid Metab. 1349, 72–80.
Pilcher, K.E., Gaudet, P., Fey, P., Kowal, A.S., Chisholm, R.L., 2007. A general purpose method for extracting RNA from Dictyostelium cells. Nat. Protoc. 2, 1329–1332.
Plak, K., Veltman, D., Fusetti, F., Beeksma, J., Rivero, F., Van Haastert, P.J., Kortholt, A., 2013. GxcC connects Rap and Rac signaling during Dictyostelium development. BMC Cell Biol. 14, 6.
Rajendran, G., Dutta, D., Hong, J., Paul, A., Saha, B., Mahato, B., Ray, S., Home, P., Ganguly, A., Weiss, M.L., 2013. Inhibition of protein kinase C signaling maintains rat embryonic stem cell pluripotency. J. Biol. Chem. 288, 24351–24362.
Robert, X., Gouet, P., 2014. Deciphering key features in protein structures with the new ENDscript server. Nucl. Acids Res. 42, W320–W324 (gku316).
Roberts, N.A., Marber, M.S., Avkiran, M., 2004. Specificity of action of bisindolylmaleimide protein kinase C inhibitors: do they inhibit the 70kDa ribosomal S6 kinase in cardiac myocytes? Biochem. Pharmacol. 68, 1923–1928.
Rosse, C., Linch, M., Kermorgant, S., Cameron, A.J., Boeckeler, K., Parker, P.J., 2010. PKC and the control of localized signal dynamics. Nat. Rev. Mol. Cell Biol. 11, 103–112.
Saran, S., Meima, M.E., Alvarez-Curto, E., Weening, K.E., Rozen, D.E., Schaap, P., 2002. cAMP signaling in Dictyostelium. J. Muscle Res. Cell Motil. 23, 793–802.
Schmittgen, T.D., Livak, K.J., 2008. Analyzing real-time PCR data by the comparative CT method. Nat. Protoc. 3, 1101–1108.
Schultz, J., Milpetz, F., Bork, P., Ponting, C.P., 1998. SMART, a simple modular architecture research tool: identification of signaling domains. Proc. Natl. Acad. Sci. 95, 5857–5864.
Siegert, F., Weijer, C.J., 1995. Spiral and concentric waves organize multicellular Dictyostelium mounds. Curr. Biol. 5, 937–943.
Sievers, F., Wilm, A., Dineen, D., Gibson, T.J., Karplus, K., Li, W., Lopez, R., McWilliam, H., Remmert, M., Söding, J., 2011. Fast, scalable generation of high-quality protein multiple sequence alignments using Clustal Omega. Mol. Syst. Biol. 7, 539.
Simpson, P.A., Spudich, J.A., Parham, P., 1984. Monoclonal antibodies prepared against Dictyostelium actin: characterization and interactions with actin. J. Cell Biol. 99, 287–295.
Steinberg, S.F., 2008. Structural basis of protein kinase C isoform function. Physiol. Rev. 88, 1341–1378.
Tabuse, Y., Izumi, Y., Piano, F., Kemphues, K.J., Miwa, J., Ohno, S., 1998. Atypical protein kinase C cooperates with PAR-3 to establish embryonic polarity in *Caenorhabditis elegans*. Development 125, 3607–3614.
Tan, S., Parker, P., 2003. Emerging and diverse roles of protein kinase C in immune cell signalling. Biochem. J. 376, 545–552.
Tang, Y., Gomer, R.H., 2008. CnrN regulates Dictyostelium group size using a counting factor-independent mechanism. Commun. Integr. Biol. 1, 185–187.
Thomason, P.A., Brazill, D.T., Cox, E.C., 2006. A series of Dictyostelium expression vectors for recombination cloning. Plasmid 56, 145–152.
Toullec, D., Pianetti, P., Coste, H., Bellevergue, P., Grand-Perret, T., Ajakane, M., Baudet, V., Boissin, P., Boursier, E., Loriolle, F., 1991. The bisindolylmaleimide GF 109203X is a potent and selective inhibitor of protein kinase C. J. Biol. Chem. 266, 15771–15781.
Veltman, D.M., Keizer-Gunnik, I., Van Haastert, P.J., 2008. Four key signaling pathways mediating chemotaxis in *Dictyostelium discoideum*. J. Cell Biol. 180, 747–753.
Wang, B., Kuspa, A., 2002. CulB, a putative ubiquitin ligase subunit, regulates prestalk cell differentiation and morphogenesis in Dictyostelium spp. Eukaryot. Cell 1, 126–136.
Weijer, C.J., 2004. Dictyostelium morphogenesis. Curr. Opin. Genet. Dev. 14, 392–398.
Wiles, N., 2005. Identification of Regulatory Binding Sites and Corresponding Transcription Factors Involved in the Developmental Control of 5′-Nucleotidase Expression in *Dictyostelium discoideum*. Department of Biological Sciences, Virginia Polytechnic Institute and State University.
Williams, J.G., 2006. Transcriptional regulation of Dictyostelium pattern formation. EMBO Rep. 7, 694–698.
Wong, E., Yang, C., Wang, J., Fuller, D., Loomis, W.F., Siu, C.-H., 2002. Disruption of the gene encoding the cell adhesion molecule DdCAD-1 leads to aberrant cell sorting and cell-type proportioning during Dictyostelium development. Development 129, 3839–3850.
Woznica, D., Knecht, D.A., 2006. Under-agarose Chemotaxis of *Dictyostelium discoideum*, *Dictyostelium discoideum* Protocols. Springer, pp. 311–325.
Zigmond, S.H., Joyce, M., Borleis, J., Bokoch, G.M., Devreotes, P.N., 1997. Regulation of actin polymerization in cell-free systems by GTPγS and Cdc42. J. Cell Biol. 138, 363–374.